# Memory Effect Manifested by a Boson Peak in Metallic Glass

P. Luo,[1] Y. Z. Li,[1] H. Y. Bai,[1] P. Wen,[1,*] and W. H. Wang[1,†]
*Institute of Physics, Chinese Academy of Sciences, Beijing 100190, People's Republic of China*

(Received 1 December 2015)

We explore the correlation between a boson peak and structural relaxation in a typical metallic glass. Consistent with enthalpy recovery, a boson peak shows a memory effect in an aging-and-scan procedure. Single-step isothermal aging produces a monotonic decrease of enthalpy and boson peak intensity; for double-step isothermal aging, both enthalpy and boson peak intensity experience, coincidently, an incipient increase to a maximum and a subsequent decrease toward the equilibrium state. Our results indicate a direct link between slow structural relaxation and fast boson peak dynamics, which presents a profound understanding of the two dynamic behaviors in glass.

DOI:

Metallic glasses have distinctive performance in mechanics and magnetics with respect to their crystalline counterparts. With a simple atomic packing, metallic glass offers an effective model system for the study of some controversial issues in glass science [1]. Because of its nonequilibrium nature, glass is continually relaxing toward a metastable equilibrium state, i.e., physical aging [2]. The modeling of glass aging and understanding its basic mechanisms is fraught with difficulty due to the complex dynamics [3–10]. One peculiar phenomenon of glass aging is the memory effect, viz., during the relaxation toward its equilibrium state. A previously aged glass often shows temporary neglect of its future (the equilibrium state) and a memory of its past, revealing history-dependent behaviors [11–15]. The memory effect is another manifestation of structural relaxation and ensures the proper description of the relaxation dynamics and, thus, procures a deeper understanding of the complex glassy-state dynamics [2,15].

Glass puzzles us not only with the localized complex atomic rearrangement arising from its nonequilibrium nature but also with the peculiar low-frequency (terahertz region) enhancement of vibrational density of states as compared with the Debye square-frequency law. This excess contribution to the vibrational spectrum is called the boson peak [16] and can be reflected in the heat capacity $C_p$ by a maximum over the Debye $T^3$ law in the temperature ($T$) dependence of $C_p/T^3$ at 5–30 K [17]. Despite the controversy, quasilocalized transverse vibrational modes associated with defective soft local structures are generally accepted as the origin of a boson peak [18–20]. A number of models have been proposed for further atomistic description of the structural origin of the anomalous low-frequency excited states, for example, soft anharmonic potentials [21–23], a transition from a minima-dominated to a saddle-dominated phase [24] or strongly anharmonic transitions between local minima of the energy landscape [25], randomly fluctuating density [26] and/or elastic constants [27], low-dimensional atomic chains [28], interstitialcylike "defects" [29], independent localized harmonic model involved in Einstein-type vibrations [30], and smeared out van Hove singularities [31,32]. Regardless of their specific assumptions and interpretations, these models are commonly related to the heterogeneous nature of glass with spatially distributed distinct subensembles contributing an excess of vibrational density of states.

Some tentative efforts have been made to explore the relationship between the structural relaxation and boson peak behavior by numerical simulations. For example, based on the potential energy landscape (PEL) [33], it was found that the boson peak intensity is positively correlated with the energy of inherent structure (local minima of PEL) [24]. The simulation showed that an observed negative correlation between the fragility of the glass-forming liquid and the boson peak intensity suggested a possible link between the structural relaxation and the boson peak dynamics [18], whereas a compelling positive correlation between the slow structural relaxation and the fast boson peak dynamics has not been investigated experimentally in a glassy state, which is of paramount importance in discriminating between these theoretical models.

In this Letter, we trace the evolution of the boson heat capacity peak with the structural relaxation manifested by the relative enthalpy change. Upon single-step isothermal aging at a constant temperature, both enthalpy and boson peak intensity show a monotonic decrease toward the metastable equilibrium state. When the sample was first aged at a certain temperature and then stepped up to a higher one, an obvious nonmonotonic behavior emerged not only in the enthalpy but also, intriguingly, in the boson peak intensity; i.e., the memory effect was revealed. The memory effect manifested by the boson peak behavior indicates clearly a direct link between the slow structural relaxation and the fast boson peak dynamics and brings a new perspective to the memory effect and the dynamics in glass.

The $Zr_{50}Cu_{40}Al_{10}$ bulk metallic glass (BMG) was prepared by suck casting from master alloy ingots to a copper mold cooled by water in an arc furnace. The amorphous nature was examined by x-ray diffraction. Calorimetric measurements and isothermal aging of the samples were performed within a Perkin-Elmer differential scanning calorimetry (DSC 8000) in high-purity standard aluminum crucibles under a constant flow of high-purity argon gas (20 ml/ min). The glass transition temperature $T_g$ and crystallization temperature $T_x$ at a heating rate of 40 K/ min were 703 and 795 K, respectively. The low temperature heat capacity $C_p$ was measured with a Quantum Design physical property measurement system, in the temperature range of 2–40 K. The samples, 2 mm in diameter with mass of around 20 mg, were carefully polished for good thermal contact and placed on top of a sapphire block of known heat capacity with a thermal grease to ensure good thermal contact. Prior to the sample measurement, we measured the heat capacity of an empty sapphire crystal with the applied grease for a baseline correction. For the enthalpy relaxation experiments, BMG disks with mass of around 150 mg were cut from a rod of 5 mm in diameter and carefully polished for good thermal contact.

We compared the time evolution of the enthalpy recovery and boson heat capacity peak in samples during single- and double-step isothermal aging. The aging protocols are schematically illustrated in Fig. S1 in the Supplemental Material [34]. For the single-step aging [Fig. S1(a) [34]], the BMG sample was first heated up from room temperature (RT) to 748 K (in the supercooled liquid temperature region) at 40 K/ min and then cooled down to RT at 80 K/ min to erase the thermal history from the preparation. A calorimetric scan at 40 K/ min was then carried out to determine the reference heat flow curve of the sample previously cooled from 748 K at 80 K/ min. The sample was then cooled from 748 K to the aging temperature $T_a = 688$ K at 80 K/ min and held for an aging time $t_a$ and then cooled down to RT at 80 K/ min. Finally, a calorimetric scan at 40 K/ min was carried out to measure the heat flow of the aged sample. The double-step aging [Fig. S1(b) [34]] involved a preaging step at temperature $T_0$ for time $t_0$, after which the temperature was stepped up to $T_a = 688$ K at 80 K/ min. The amorphous nature of the aged samples was ensured by measuring the enthalpy of crystallization and XRD.

Figure 1 plots the enthalpy recovery heat flow curves after single- and double-step isothermal aging. During the single-step aging [Fig. 1(a)], as $t_a$ increases, the endothermal peak becomes enhanced and broadens, showing a typical structural relaxation of glass [2], while for the double-step aging [Fig. 1(b)], as the sample was preaged at a lower temperature before the second step aging, the endothermal peak first decreased and then increased with $t_a$. The relative enthalpy change $\Delta H$ can be calculated by subtracting the temperature integral of the heat flow curve of the aged state from that of the reference state. As shown in the inset of Fig. 1(a), during the single-step aging (see the solid red line), the relative enthalpy change $\Delta H$ as a function of $t_a$ decreases monotonically toward the equilibrium value [shown by curve $A$ in Fig. 3(a)], while the double-step aging [see the dashed green line in the inset of Fig. 1(a)] produces a nonmonotonic evolution of the $\Delta H$ with $t_a$ [curve $C$ in Fig. 3(a)].

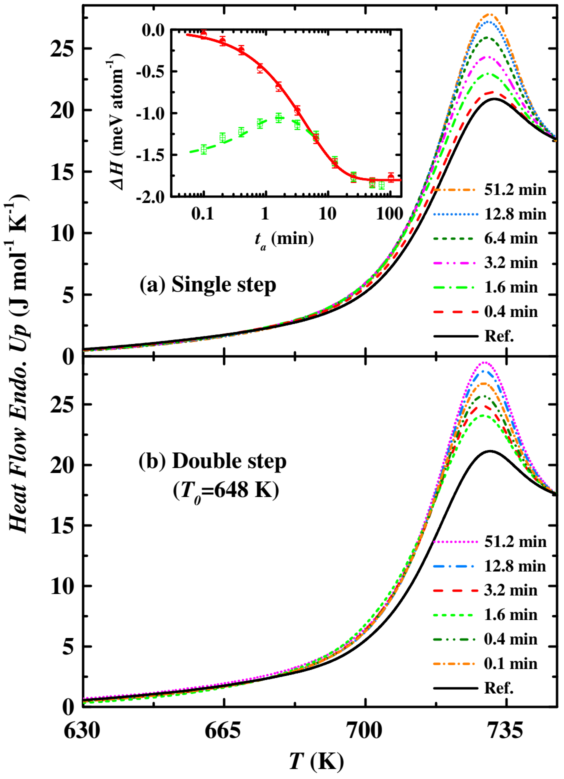

FIG. 1. Enthalpy recovery after (a) single-step isothermal aging and (b) double-step isothermal aging for different aging times $t_a$, $T_a = 688$ K for all cases. For the double-step aging $T_0 = 648$ K and $t_0 = 20$ min. The black solid lines represent the reference curve (Ref.) without isothermal aging. The inset in (a) is the relative enthalpy change $\Delta H$ against the $t_a$; the lines are a guide for the eyes; the solid red line is for the single-step aging and the dashed green line is for the double-step aging.

The aging protocol of the samples for low-$T$ heat capacity measurements was similar to, yet slightly different from, the enthalpy measurements (Fig. S1 [34]). The sample was heated up from RT to 748 K at 40 K/ min and then immediately cooled down to the aging temperature ($T_a$ for single-step aging or $T_0$ for double-step aging) at 80 K/ min, without the second and last up-scans to measure the heat flow. Figure 2 plots the measured low-$T$ heat capacity of the aged samples as $(C_p\text{-}C_p^{\text{cryst}})/T^3$ vs $T$, making visible the boson peak contribution. $C_p^{\text{cryst}}$ represents the measured low-$T$ heat capacity of the crystalline $\mathrm{Zr_{50}Cu_{40}Al_{10}}$ sample which was obtained by heating the glassy sample to 823 K and held for 3 min for full crystallization. $C_p^{\text{cryst}}$ shows no contribution to the boson peak but a considerable heat capacity from electronic and lattice contributions; thus, it can be subtracted from that of

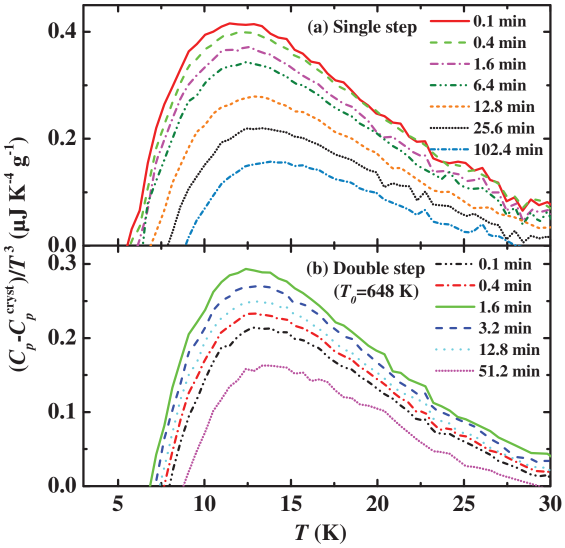

FIG. 2. Boson heat capacity peaks of samples from (a) single- and (b) double-step isothermal aging for different aging times $t_a$, $T_a = 688$ K for all cases. For the double-step aging $T_0 = 648$ K and $t_0 = 20$ min.

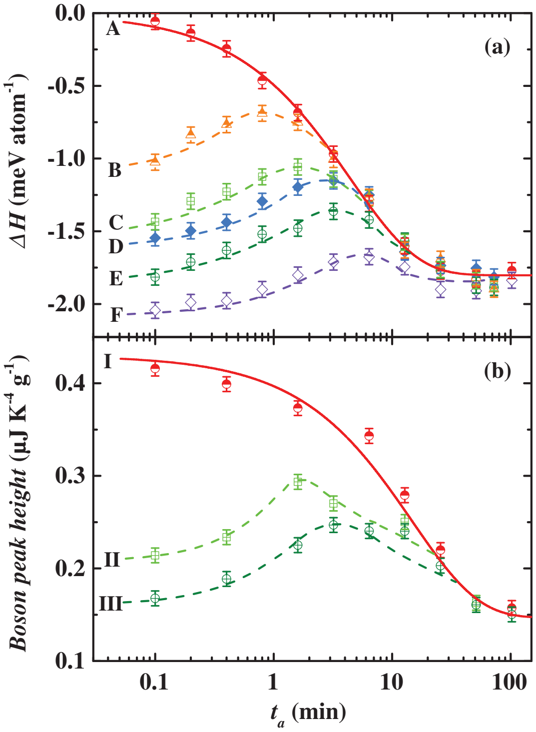

FIG. 3. (a) Relative enthalpy change $\Delta H$ against the aging time $t_a$ for single-step (curve *A*) and double-step isothermal aging (curves *B*–*F*). For double-step aging, the preaging temperatures $T_0$ for cases *B*–*E* were 638, 648, 658, and 668 K, respectively, and the preaging time $t_0 = 20$ min. Case *F* with $T_0 = 668$ K and $t_0 = 30$ min. (b) Boson peak height against the $t_a$ for single- (curve I) and double-step isothermal aging ($T_0 = 648$ K for curve II and $T_0 = 668$ K for curve III, $t_0 = 20$ min). $T_a = 688$ K for all cases. The lines are drawn as a guide for the eyes.

the glass to highlight the boson peak contribution. Figure 2(a) shows the boson peak of the samples after single-step aging; it becomes more and more depressed as $t_a$ increases, and the peak maximum shifts to higher $T$ by ~2 K with $t_a$ increasing from 0.1 to 102.4 min. Such aging effect on the boson peak accords with previous observations in other BMGs [35–38]. Figure 2(b) shows the boson peak after double-step aging; remarkably, as $t_a$ increases, it first becomes more and more pronounced and then depressed, showing a nonmonotonic evolution. For both single- and double-step aging, it is clear that with the higher strength of the boson peak, the peak maximum occurs at the lower temperature.

Figure 3 plots the $t_a$-dependent relative enthalpy change $\Delta H$ [Fig. 3(a)] and boson peak height [peak maximum of $(C_p\text{-}C_p{}^{\text{cryst}})/T^3$, Fig. 3(b)] for various aging protocols. During single-step aging, the $\Delta H$ [curve *A* in Fig. 3(a)] and the boson peak height [curve I in Fig. 3(b)] decrease monotonically until the metastable equilibrium state is attained after around 100 min, showing a typical aging effect. Nevertheless, as the glass was preaged at a lower temperature $T_0$, i.e., with additional thermal history endowed, the structural relaxation behavior turned to exhibit a totally different manner [see curves *B*–*F* in Fig. 3(a)]. The $t_a$-dependent $\Delta H$ undergoes first an increase moving away from the equilibrium value to a maximum followed by a decrease approaching it, showing a temporary neglect of the equilibrium state; thus, the memory effect is revealed. And, the $\Delta H$ peak maximum occurs later as the preaging temperature $T_0$ or the preaging time $t_0$ increases. Figure 3(b) also shows the surprising result that for double-step aging (curves II and III), the $t_a$-dependent boson peak height experiences an incipient increase to a maximum and a following decrease to merge with that of the single-step aging within the experimental sensitivity. For curve II, with $T_0 = 648$ K and $t_0 = 20$ min, the boson peak height value peaks at around $t_a = 1.6$ min, in agreement with curve *C* in Fig. 3(a) under the same aging protocol. Likewise, the magnitude of the boson peak [curve III in Fig. 3(b)] and relative enthalpy change $\Delta H$ [curve *E* in Fig. 3(a)] follow similar evolution and peak simultaneously at around $t_a = 3.2$ min for the double-step aging of $T_0 = 668$ K and $t_0 = 20$ min. All in all, the boson peak, which reflects the anomaly in the frequency spectra of atomic vibration in amorphous materials, shows obvious history-dependent behaviors of the memory effect and behaves akin to the structural relaxation manifested from enthalpy measurements.

In Fig. 4, the boson peak height vs $\Delta H$ is plotted. Within the accuracy limit of the method of measuring the boson peak behavior, Fig. 4 shows that the boson peak intensity follows an almost linear relationship with the relative enthalpy change. The result allows a semiquantitative construction of the correlation between the structural

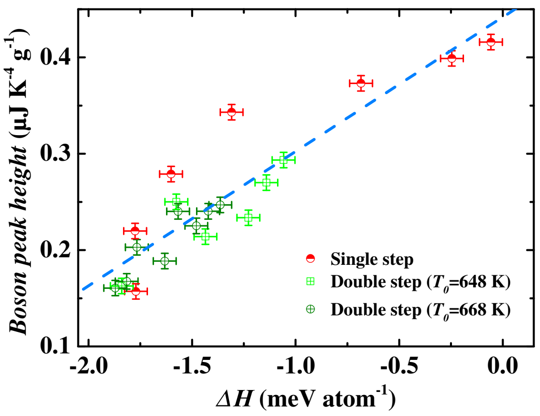

FIG. 4. Relationship between the boson peak height and the relative enthalpy change; the data from both single- and double-step aging are embraced. The dashed line gives a guide for the eyes.

relaxation and boson peak behavior. The clear-cut experimental observation has been given that the boson peak behaves in line with the relative enthalpy change during not only the single-step but also the double-step isothermal aging, strongly indicating a close correlation between the slow structural relaxation and the fast boson peak dynamics in metallic glass. It is highly reminiscent of the observation by Grigera *et al.* [24] that the sampling of higher energy on the potential energy landscape leads to an increase in the boson peak intensity. Structurally, the simulation by Shintani and Tanaka [18] shows that large local (free) volume benefits the local boson peak intensity over the Debye value. Recent works reveal that the boson peak intensity of severely deformed metallic glasses can be strongly enhanced due to the formation of shear bands with excess free volume [35,36]. Starting from this scenario, the appearance of the memory effect during the double-step aging can be understood.

Phenomenological or semiquantitative models have been employed to describe the relaxation dynamics with emphasis on the memory effect, for example, the two-relaxation-time model [11], a combination of chemical and topological structural relaxation [12], and the activation energy spectrum model [15]. These models for the understanding of the memory effect are commonly based on the spatially randomly distributed local regions, within which the atomic motions can be detected and appear as secondary relaxations [39]. Because of the heterogeneous nature of glass, distinct local regions show enhanced or reduced mobility with respect to the average relaxation rate, resulting in a concomitant dispersion of relaxation times [5,6,9,10]. Within the heterogeneous dynamics scenario, the memory effect can be described in terms of the nonexponential relaxation function [2] but without giving a clear microscopic physical picture. The boson peak is also closely related to the soft localized regions [18–20]. Based on the activation energy spectrum model [15], the microscopic picture concerning the memory effect can be drawn. Flow units are any available and thermally (or mechanically) activated localized rearrangement [39,40]. At the lower temperature $T_0$, the flow units with low activation energy come to be depleted (achieving metastable equilibrium). At the higher temperature $T_a$, the reactivation of these flow units takes place, resulting in the observed increase in enthalpy and boson peak intensity. The flow units with high activation energy are still active at $T_0$, and at $T_a$, further rearrangement continues resulting in the decrease of the enthalpy and boson peak, and the reactivated flow units will, subsequently, return again to the metastable equilibrium; thus, a nonmonotonic behavior was observed. The higher preaging temperature $T_0$ and/or preaging time $t_0$ results in the depletion of more flow units with high activation energy, and it takes more time for these flow units to be reactivated at $T_a$, so we observe the values of $\Delta H$ and the boson peak intensity peak at longer $t_a$ (see Fig. 3).

Here arises a question of how a temperature rise brings about the reactivation of the originally depleted flow units. A recent work by Ketov *et al.* [41] provides new insight that the thermal cycling of metallic glass to cryogenic temperatures causes atomic-scale structural rejuvenation. At low temperatures, the effect of aging can be reduced, and the temperature change will induce internal stresses that cause atomic-scale nonaffine deformation. Remarkably, the thermal cycling of partially relaxed BMGs can induce an increased fraction of flow units and better plasticity than that of as-cast BMGs [41], suggesting that large as-cast heterogeneities (soft liquidlike regions) are prone to absorb a portion of the newly induced internal stresses. Structural relaxation has been proposed to be driven by atomic-scale internal stress [7,10], while as the thermal expansion coefficient of flow units varies from that of their neighbors, the originally depleted flow units are cast again into an incompatible stress environment as the temperature is elevated, resulting in additional internal stresses that bring back the BMG to a higher energy state. With the energy of inherent structure being the relevant control parameter [24], an increase of the boson peak intensity is observed.

Recent x-ray photo correlation spectroscopy studies on the aging of metallic glasses gives more atomic-scale details [42]. Following both dynamical and structural approaches, it pointed out that microscopic aging in fast-quenched metallic glasses can be ascribed to two processes: the first one which affects the density until the density inhomogeneities are completely released; the second one is an ordering on the medium range, which does not affect the density [42–44]. This scenario enables a clearer interpretation of our results. These two processes act together during the lower temperature fast aging step, which releases a good part of inhomogeneities by the annihilation of flow units with lower activation barriers, and the glass attains microscopically a relatively homogeneous state [45]. As the glass is stepped quickly to higher temperatures, a mismatch of the thermal expansion coefficient between neighboring local regions (medium range) induces new internal stresses that cause transient local disordering by atomic rearrangement (rejuvenation). While the second process of medium-range ordering still goes on at the higher temperature step and the nonmonotonic behavior results. From this point of view, the memory effect is one corollary of the heterogeneous nature of glasses and directly comes from a transient local disordering accompanied by an enhancement in the boson peak intensity, which is an intrinsically universal feature of glasses and has been widely believed to originate from local soft regions [18–20].

In conclusion, through the memory effect, we bridge the structural relaxation and the universal boson peak feature in a typical Zr-based BMG. Consistent with enthalpy relaxation, the boson peak shows a memory effect. The observed contrasting monotonic versus nonmonotonic relaxation behavior of the enthalpy and boson peak intensity in the single- and double-step aging, respectively, univocally indicates a close correlation between the slow structural relaxation and the fast boson peak dynamics. The results benefit the understanding of the history-dependent behaviors of the memory effect and the anomalous low-energy excitation in glass.

We thank M. X. Pan, D. Q. Zhao, Z. Lu, and W. C. Xiao for experimental assistance and discussions. This work was supported by the NSF of China (Grant No. 51271195) and MOST 973 Program (Grant No. 2015CB856800).

---

[*] Corresponding author.
pwen@iphy.ac.cn

[†] Corresponding author.
whw@iphy.ac.cn

[1] W. H. Wang, J. Appl. Phys. **99**, 093506 (2006).
[2] I. M. Hodge, J. Non-Cryst. Solids 169 164 (1994).
[3] K. L. Ngai, *Relaxation and Diffusion in Complex Systems* (Springer, New York, 2011).
[4] L. Berthier and G. Biroli, Rev. Mod. Phys. **83**, 587 (2011).
[5] J. C. Mauro, S. S. Uzun, and S. Sen, Phys. Rev. Lett. **102**, 155506 (2009).
[6] R. Richert, Phys. Rev. Lett. **104**, 085702 (2010).
[7] B. Ruta, Y. Chushkin, G. Monaco, L. Cipelletti, E. Pineda, P. Bruna, V. M. Giordano, and M. Gonzalez-Silveira, Phys. Rev. Lett. **109**, 165701 (2012).
[8] C. Brun, F. Ladieu, D. L'Hôte, G. Biroli, and J.-P. Bouchaud, Phys. Rev. Lett. **109**, 175702 (2012).
[9] M. Paluch, Z. Wojnarowska, and S. Hensel-Bielowka, Phys. Rev. Lett. **110**, 015702 (2013).
[10] Z. Evenson, B. Ruta, S. Hechler, M. Stolpe, E. Pineda, I. Gallino, and R. Busch, Phys. Rev. Lett. **115**, 175701 (2015).
[11] A. L. Greer and J. A. Leake, J. Non-Cryst. Solids **33**, 291 (1979).
[12] A. van den Beukel, S. Van der Zwaag, and A. L. Mulder, Acta Metall. **32**, 1895 (1984).
[13] D. P. B. Aji, P. Wen, and G. P. Johari, J. Non-Cryst. Solids **353**, 3796 (2007).
[14] C. A. Volkert and F. Spaepen, Acta Metall. **37**, 1355 (1989).
[15] M. R. J. Gibbs, J. E. Evetts, and J. A. Leake, J. Mater. Sci. **18**, 278 (1983).
[16] B. Frick and D. Richter, Science **267**, 1939 (1995).
[17] *Amorphous Solids: Low Temperature Properties*, edited by W. A. Phillips (Springer-Verlag, Berlin, 1981).
[18] H. Shintani and H. Tanaka, Nat. Mater. **7**, 870 (2008).
[19] H. R. Schober, J. Non-Cryst. Solids **357**, 501 (2011).
[20] B. B. Laird and H. R. Schober, Phys. Rev. Lett. **66**, 636 (1991).
[21] V. G. Karpov *et al.*, Zh. Eksp. Teor. Fiz. **84**, 760 (1983).
[22] U. Buchenau, Y. M. Galperin, V. L. Gurevich, D. A. Parshin, M. A. Ramos, and H. R. Schober, Phys. Rev. B **46**, 2798 (1992).
[23] L. Gil, M. A. Ramos, A. Bringer, and U. Buchenau, Phys. Rev. Lett. **70**, 182 (1993).
[24] T. S. Grigera, V. Martín-Mayor, G. Parisi, and P. Verrocchio, Nature (London) **422**, 289 (2003).
[25] V. Lubchenko and P. G. Wolynes, Proc. Natl. Acad. Sci. U.S.A. **100**, 1515 (2003).
[26] S. R. Elliott, Europhys. Lett. **19**, 201 (1992).
[27] W. Schirmacher, G. Ruocco, and T. Scopigno, Phys. Rev. Lett. **98**, 025501 (2007).
[28] H. R. Schober and C. Oligschleger, Phys. Rev. B **53**, 11469 (1996).
[29] A. N. Vasiliev, T. N. Voloshok, A. V. Granato, D. M. Joncich, Y. P. Mitrofanov, and V. A. Khonik, Phys. Rev. B **80**, 172102 (2009).
[30] M. B. Tang, H. Y. Bai, and W. H. Wang, Phys. Rev. B **72**, 012202 (2005).
[31] S. N. Taraskin, Y. L. Loh, G. Natarajan, and S. R. Elliott, Phys. Rev. Lett. **86**, 1255 (2001).
[32] A. I. Chumakov *et al.*, Phys. Rev. Lett. **106**, 225501 (2011).
[33] F. H. Stillinger, Science **267**, 1935 (1995).
[34] See the Supplemental Material at http://link.aps.org/supplemental/10.1103/PhysRevLett.000.000000 for experimental details and additional information.
[35] J. Bünz, T. Brink, K. Tsuchiya, F. Meng, G. Wilde, and K. Albe, Phys. Rev. Lett. **112**, 135501 (2014).
[36] Y. P. Mitrofanov, M. Peterlechner, S. V. Divinski, and G. Wilde, Phys. Rev. Lett. **112**, 135901 (2014).
[37] Y. Li, P. Yu, and H. Y. Bai, J. Appl. Phys. **104**, 013520 (2008).
[38] B. Huang, H. Y. Bai, and W. H. Wang, J. Appl. Phys. **115**, 153505 (2014).
[39] P. Luo, Z. Lu, Z. G. Zhu, Y. Z. Li, H. Y. Bai, and W. H. Wang, Appl. Phys. Lett. **106**, 031907 (2015); H. B. Yu *et al.*, Natl. Sci. Rev. **1**, 429 (2014).
[40] Z. Wang, B. A. Sun, H. Y. Bai, and W. H. Wang, Nat. Commun. **5**, 5823 (2014).
[41] S. V. Ketov *et al.*, Nature (London) **524**, 200 (2015).
[42] V. M. Giordano and B. Ruta, Nat. Commun. **7**, 10344 (2016).
[43] J. Bednarcik, C. Curfs, M. Sikorski, H. Franz, and J. Z. Jiang, J. Alloys Compd. **504~~S~~**, S155 (2010).
[44] M. Mao, Z. Altounian, and R. Brüning, Phys. Rev. B **51**, 2798 (1995).
[45] P. Luo, Z. Lu, Y. Z. Li, H. Y. Bai, P. Wen, and W. H. Wang, Phys. Rev. B **93**, 104204 (2016).